Structure of the Highly Conserved *HERC2* Gene and of Multiple Partially Duplicated Paralogs in Human

Yonggang Ji,[3] Nancy A. Rebert, John M. Joslin,[1] Michael J. Higgins,[2]
Roger A. Schultz,[1] and Robert D. Nicholls[4]

Department of Genetics, Case Western Reserve University School of Medicine, and Center for Human Genetics, University Hospitals of Cleveland, Cleveland, Ohio 44106-4955 USA; [1]The McDermott Center for Human Growth and Development, and Department of Pathology, University of Texas Southwestern Medical Center, Dallas, Texas 75235 USA; [2]Department of Cancer Genetics, Roswell Park Cancer Institute, Buffalo, New York 14263 USA

Recombination between chromosome-specific low-copy repeats (duplicons) is an underlying mechanism for several genetic disorders. Recently, a chromosome 15 duplicon was discovered in the common breakpoint regions of Prader–Willi and Angelman syndrome deletions. We identified previously the large *HERC2* transcript as an ancestral gene in this duplicon, with ~11 *HERC2*-containing duplicons, and demonstrated that recessive mutations in mouse *Herc2* lead to a developmental syndrome, juvenile development and fertility 2 (*jdf2*). We have now constructed and sequenced a genomic contig of *HERC2*, revealing a total of 93 exons spanning ~250 kb and a CpG island promoter. A processed ribosomal protein L41 pseudogene occurs in intron 2 of *HERC2*, and putative VNTRs occur in intron 70 (28 copies, ~76-bp repeat) and 3′ exon 40 through intron 40 (6 copies, ~62-bp repeat). Sequence comparisons show that *HERC2*-containing duplicons have undergone several deletion, inversion, and dispersion events to form complex duplicons in 15q11, 15q13, and 16p11. To further understand the developmental role of *HERC2*, a highly conserved *Drosophila* ortholog was characterized, with 70% amino acid sequence identity to human HERC2 over the carboxy-terminal 743 residues. Combined, these studies provide significant insights into the structure of complex duplicons and into the evolutionary pathways of formation, dispersal, and genomic instability of duplicons. Our results establish that some genes not only have a protein coding function but can also play a structural role in the genome.

[The sequence data described in this paper have been submitted to GenBank under accession nos. AF189221 (*Drosophila HERC2* partial cDNA), AC004583 (human *HERC2* exons 1–52, genomic); AF224242–AF224257 (human *HERC2* exons 54–70, partial genomic sequences); AF225400–AF225409 (human *HERC2* exons 71–93, partial genomic sequences). The exon-intron boundaries for exons 53–93 are derived from BACs R-142A11 and 263O22. Additional information is available as a supplementary table at www.genome.org.]

Although the underlying genetic defects in Prader–Willi syndrome (PWS) and Angelman syndrome (AS) are aberrations in imprinted gene expression, the majority of patients carry a cytogenetic deletion of chromosome 15q11–q13 (Nicholls et al. 1998). Low-copy repeats, or duplicons, have been mapped to the common deletion breakpoint regions (Buiting et al. 1998; Amos-Landgraf et al. 1999; Christian et al. 1999; Y. Ji, E. Eichler, S. Schwartz, and R.D. Nicholls, in prep.), including a large gene (*HERC2*) and partially duplicated paralogs, many copies of which are actively transcribed (Ji et al. 1999). The ancestral *HERC2* gene gives rise to a 15.3-kb mRNA, and the duplicated paralogs to a family of 6- to 7-kb transcripts (Amos-Landgraf et al. 1999; Ji et al. 1999). The functional *HERC2* gene was mapped just distal of *P*, suggesting the origin of the duplications in 15q13 (Fig. 1a; Ji et al. 1999). Several other ESTs also occur either within some *HERC2*-containing or independent duplicons but have not been characterized in detail (Christian et al. 1999). The duplicons containing *HERC2* have undergone multiple genomic duplication events, resulting in at least 12 copies of partially duplicated segments, with 7 copies located at or close to the two proximal (15q11) deletion breakpoints, 3 copies at the distal (15q13) breakpoint, and 2 additional copies at the pericentromeric region of chromosome 16p (Buiting et al. 1998; Amos-Landgraf et al. 1999). The 15q11 and 15q13 duplicons (Fig. 1a) have been termed the *END* repeats because

[3]*Present address: Genentech, Inc., Department of Bioinformatics, South San Francisco, California 94080 USA.*
[4]**Corresponding author.**
E-MAIL rxn19@po.cwru.edu; FAX (216) 368-3432.

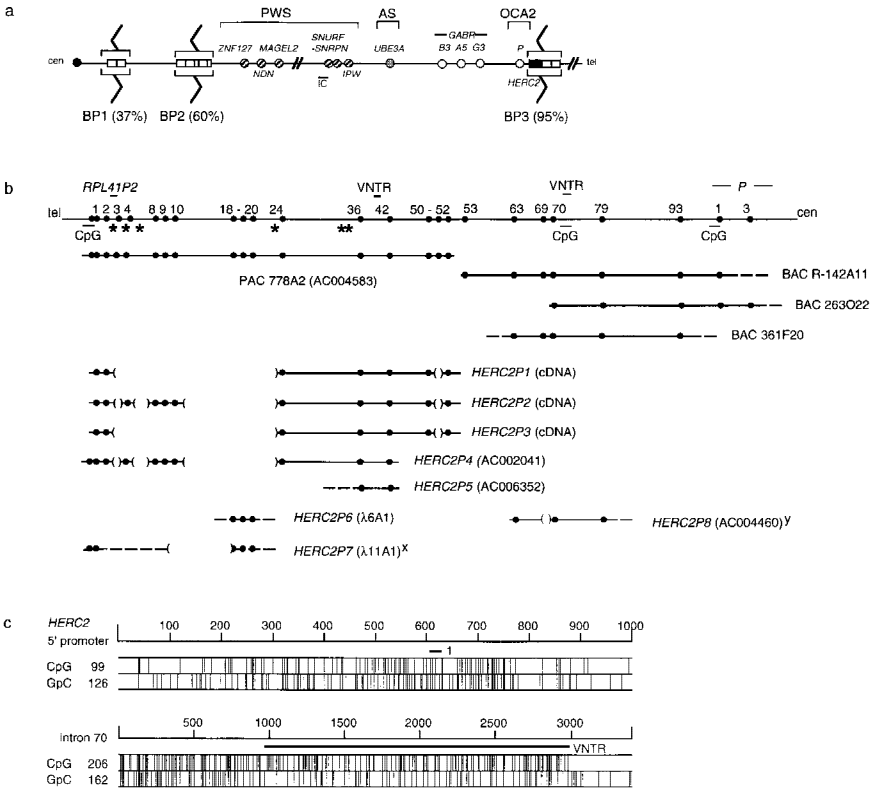

Figure 1 Genomic characterization of *HERC2* and partially duplicated paralogs. (*a*) Model showing the position of *HERC2*-containing duplicons (□; *HERC2*, ■) in chromosomes 15q11 and 15q13. These map close to or within breakpoint 2 (BP2) and BP3, whereas those shown hypothetically at BP1 are only known to map centromeric of BP2 (Amos-Landgraf et al. 1999). The frequency (%) of breakpoints (zigzag lines) at each location is shown. PWS, AS, and OCA2 are the three known disease loci in 15q11–q13 (Nicholls et al. 1998). Other symbols: (cen) centromere; (circles) genes [(hatched) paternal only; (open) nonimprinted; (shaded) maternal only]; (IC) imprinting center; (tel) telomere. (*b*) Genomic map with PAC/BAC clone contig of the *HERC2* locus and comparison to eight of the duplicated loci. Numbers at *top* correspond to exon numbers of *HERC2* (several exons of the flanking *P* gene, two VNTRs, and the *RPL41P2* gene are also shown). (CpG) CpG islands; (*) simple repeats of five or more copies in 5′ *HERC2* (see Table 1). Broken lines represent an unknown extent for that particular end of a clone; parentheses [( )] represent genomic deletions of *HERC2* in each duplicon. (^{x}) Intron 9 and exon 18 are joined together in this clone; (^{y}) sequence homologous to intron 55 was also identified 7 kb 5′ of exon 63 homologous sequence in this clone. (*c*) CpG content of the *HERC2* 5′ promoter region (nucleotide 4101–5100 of PAC 778A2 sequence) and CpG island upstream and spanning the intron 70 VNTR. Exon 1 and the intron 70 putative VNTR are shown as bars.

they flank the ends of the PWS/AS region (Amos-Landgraf et al. 1999).

The large 528-kD HERC2 protein contains several motifs, including three RCC1-like domains, a carboxy-terminal HECT domain, and a ZZ-type zinc finger. HERC2 is also distantly related to HERC1 (p532) and HERC3, both of which also contain a carboxy-terminal HECT domain and at least one RCC1-like domain (Ji et al. 1999). HERC1 has been suggested to function in vesicular trafficking pathways on the basis of localization to both the cytosol and the Golgi apparatus, and interaction with clathrin heavy chain (Rosa et al. 1996; Rosa and Barbacid 1997), whereas no functional studies have been performed on HERC3 (Nomura et al. 1994). Based on the conserved motifs, mouse mutation studies, and by analogy to the related HERC1, it has been suggested that human HERC2 may act as a guanine nucleotide exchange factor and E3 ubiquitin ligase, with function in protein trafficking and degradation pathways in the cell (Ji et al. 1999). Recently, the mouse *Herc2* gene has been cloned, mutations of which were shown to cause severe developmental delay, jerky gait, sterility, and juvenile lethality in a recessively inherited manner (*jdf2*, or *rjs*; Lehman et al. 1998; Ji et al. 1999). Mutations of *HERC2* have so far not been linked to any human genetic disorder. Although PWS and AS deletion patients are hemizygous for 3′ *HERC2* (Ji et al. 1999), there is no evidence that this gene contributes to any of the PWS or AS phenotypes, consistent with a recessive gene.

To provide a framework for characterizing the role of *HERC2* in human disease and the structure and evolution of chromosome 15q11–q13 duplicons, we constructed a genomic contig spanning the *HERC2* locus and determined the exon–intron structure of *HERC2*. A highly conserved *Drosophila HERC2* ortholog was also characterized. A comparison at the genomic level of the *HERC2* structure with eight partially duplicated copies allows an understanding of the structure and evolutionary formation of several *HERC2*-containing duplicons.

RESULTS

Construction of a Genomic PAC and BAC Contig of *HERC2*

Of 30 positive PAC clones identified using a 5′ *HERC2* probe, only 1 (778A2) contained an exonic sequence tagged site (STS) identical to *HERC2*. By Southern hybridization using various 5′ *HERC2* probes, this PAC contained >7.9 kb of *HERC2* coding sequence (data not shown). In addition, it is positive for a CpG island probe homologous to a duplicated copy of *HERC2* (Amos-Landgraf et al. 1999), suggesting 778A2 contains the putative *HERC2* promoter (Fig. 1b). Three BAC clones were isolated spanning 3′ *HERC2* (see Methods), and all were positive by STS PCR for the 3′ UTR of *HERC2*, which is unique (Ji et al. 1999). Typing of other *HERC2* STSs (see Methods) and those from the *P* gene (Lee et al. 1995) showed the extent of each genomic clone (Fig. 1b). Combined with results from PAC and BAC clone sequencing (see below), the data indicate that the contig covers all *HERC2* exons, with 778A2 covering *HERC2* exons 1–52, R-142A11 exons 53 to the 3′ UTR (exon 93), 263O22 exons 70–93, and 361F20 starting 5′ of exon 63 and extending beyond exon 93 (Fig. 1b).

Genomic Organization of the *HERC2 Locus*

We have sequenced all the exon–intron boundaries of *HERC2*, which demonstrates that the 15.3-kb cDNA is encoded by 93 exons (Table 1). All exon–intron boundaries conform to the consensus splice sequences (Maquat 1996). The transcription initiation of *HERC2* is putatively under the control of a CpG-island promoter (Fig. 1c). Exon 1 is the smallest exon (30 bp), and exon 93 is the largest exon (997 bp), with an average exon size of 164 bp. The translational initiation codon ATG is in exon 2, and the stop codon (TAA) is in exon 93. Although the size of some 3′ introns has not been determined, intron size varies from 77 bp (intron 32) to 21,847 bp (intron 2). The first 52 exons, within PAC 778A2, occupy a genomic distance of 132 kb. Because the last 41 exons and introns span a minimum of ~66 kb and based on the size of 3′-*HERC2* BACs, we estimate that the *HERC2* genomic locus spans 200–250 kb.

The genomic sequence of 5′ *HERC2* (exons 1–52) has a moderate level of genome-wide repetitive elements that comprise 46% of the total sequence (SINE 21.20%, LINE 18.22%, LTR 3.48%, and other elements, 2.08%), with a GC content of 43.5%. Several simple repeats were identified, including five dinucleotide repeats with copy numbers >15, and a tetranucleotide repeat (Table 1; Fig. 1b). In addition, 43 copies of clustered TGAG were identified in intron 38, in a TG-rich region (109,548–110,202 nucleotides of PAC 778A2). We also identified two putative variable number of tandem repeat (VNTR) sequences within *HERC2*. One is located in intron 40, with six copies of an ~62-bp sequence (range 60–63), each of >90% identity (Fig. 2a). Interestingly, the first copy of this repeat starts within exon 40, and the other five copies span virtually all of intron 40. Analysis of BAC 263O22 sequence identified, in intron 70, 28 copies of an ~76-bp repeat monomer (range 64–79), each with >84% identity (Fig. 2b). This VNTR is adjacent to an intronic CpG island (Fig. 1c) that is of unknown function. With four to six CpG dinucleotides per repeat, a 3-kb CpG island can be defined that is larger than the average size for a CpG island (Bird 1986).

In comparing the 5′ (exons 1–52) genomic sequence with *HERC2* cDNA, 13 sequence changes were identified. Two were cDNA sequence errors, at positions 328 (A replaces T) and 1228 (G replaces C), neither of which changes the translated protein sequence. Eleven changes represent putative single nucleotide polymorphisms (SNPs) (Supplemental table available at www.genome.org), five of which are silent and do not affect corresponding amino acid sequences. Six would cause amino acid changes, although three occur at amino acids that differ between human and mouse and may not be significant. Of the others, one is conservative (Leu → Phe), one may be conservative (His → Arg) if a positively charged residue is sufficient here, and one is nonconservative (Ser → Arg). These putative SNPs will aid assessment of the role of *HERC2* in human disease.

A BLAST search of repeat-masked *HERC2* genomic sequence identified multiple ESTs, but most show only 84%–99% homology to the genomic sequence, suggesting that they are transcribed from *HERC2*-related duplicated segments. These ESTs can be assigned to four classes. (1) These include ESTs that contain *HERC2* exon-related sequence representing *HERC2*-related pseudogenes (Buiting et al. 1998; Ji et al. 1999), and (2) rare ESTs that contain homologous sequence to *Alu* or L1 elements, which may represent nonfunctional transcripts. A 99% homologous sequence to IMAGE clone 120151 (AF129928), identified in *HERC2* intron 4, is actually mostly part of an ancient L1 element (69.2% identity) and hence most likely does not represent a unique gene in the chromosome 15 duplicon, contrary to a previous report (Christian et al. 1999). (3) A small number of ESTs contain only unique sequence, but as these ESTs do not cluster, they may not represent new genes and, rather, reflect background transcription in the genome. (4) A processed pseudogene for ribosomal protein L41 occurs within intron 2 of *HERC2* (Fig. 1b). This *L41* pseudogene (*RPL41P2*) was inserted into the 3′ end of an *Alu* repetitive element, with a 14-bp direct repeat (AAAAAATTATCTGG) flanking both ends of the pseudogene, whereas the functional *L41* gene maps to chromosome 12 (Kenmochi et al. 1998).

Comparison of *HERC2* to Partially Duplicated Paralogs

Our characterization of the *HERC2* genomic locus now allows direct sequence comparisons to the *HERC2*-related portions of chromosome 15q11, 15q13, and 16p11.2 duplicons (see introductory section). For the *HERC2P1* and *P3* cDNA (Ji et al. 1999), *HERC2* exons 3–23 and exon 51 are deleted, whereas exons 1, 2, 24–50, and 52 are present, and exons 53–93 are absent (Fig. 1b). For *HERC2P2* (Ji et al. 1999), exons 4 and 8–10 are present as well (Fig. 1b). Most cDNA clones derived

Table 1. Exon–Intron Organization of the Human *HERC2* Gene

Exon no.	cDNA position[a]	Exon first base[b]	Intron–exon boundary	Exon size	Exon–intron boundary	Intron size[c]
1	1	4708	GAGGCG	30	CGTCAGgtcctggcct	610
2	31	5348	ttacttgcagGCCTGA	103	ATACAGgtggggtttg	21847[d]
3	134	27298	tcattgccagCTTGCA	115	GAAAAGgtaagggcct	6377[e]
4	249	33790	aattctgcagATGATA	135	AACCAGgtaatcttgt	12596
5	384	46521	tattttctagATGTGA	220	AAAAAGgtaacaataa	5062[f]
6	604	51803	tcgtctgcagTTCCCG	101	GATCAGgtacggtccc	457
7	705	52361	gtgcgcccagGCGAGG	157	GACGGGgtgagttctt	1286
8	862	53804	ttcatttcagGGATGT	111	GCTGAGgtgagggctg	507
9	973	54422	tctcctttagCCAAAT	172	ATGCACgtgagtgtca	1346
10	1145	55940	tcctttctagCTTTTG	174	CATAAGgtgtgtgtgc	1258
11	1319	57372	tatcttacagGGATCA	189	ACGCTGgtgagtgttc	631
12	1508	58192	ccttctttagGCCCCA	152	CACTGTgtatgtatcg	2490
13	1660	60834	tctccccaagGCCTTT	158	GCCATGgtacgtctgc	85
14	1818	61077	ctgtttgaagGCTCCA	114	AGAACGgtacgtagag	2448
15	1932	63639	tattttttagGGCAAG	252	TGCAAGgtgagtgcaa	1947
16	2184	65838	tcccttgtagGGAAGA	194	GCCCAGgtactgaata	3515
17	2378	69547	ttcctcttagAGCTTT	201	CTTCAGgtattcatga	743
18	2579	70491	ctcctttcagTTGCAT	229	GCGCAGgtgggcctgg	92
19	2808	70812	tctatttcagTTTCAG	125	ATCCAGgtatggcttt	1353
20	2933	72290	tgaattacagGATATT	179	TCTTAGgtaaatcgta	5603
21	3112	78072	tcctgtatagAAACAT	185	TTTCTAgtaagttgct	1653
22	3297	79910	cttcttcaagGTCCAG	156	TTACTGgtaccttttg	675
23	3453	80741	ttaaatgtagGTGTTC	186	TAATGGgtacggcgtc	7108[g]
24	3639	88035	gtatatacagAGTCAT	171	TTCTTGgtaagattac	384
25	3810	88590	tttgtttcagCTCAGT	104	TTGGAGgtgaggctgt	1000
26	3914	89694	atttttccagCCTGAC	151	GTGCCAgtaagaaaat	2676
27	4065	92521	cattttccagAATGGC	215	GTGAAGgtgagctagg	273
28	4280	93009	tctgttgcagGACTTT	133	ATTTAGgtaaggagct	102
29	4413	93244	ctttttacagGTCATG	128	ATTAAGgtgatagatt	92
30	4541	93464	aactttgcagACTCAT	196	AGAGAGgtaagaatgt	2645
31	4737	96305	taaaacacagTTCCTA	134	CCCAAGgtgcagtatt	519
32	4871	96958	cctttgttagGACAAA	174	AAACAGgtaacatttg	77
33	5045	97209	tattttgcagTTGGAG	137	TATAGGgtaaaacgtt	113
34	5182	97459	tatttgaaagGGAACC	152	AGCTTGgtgagtcaat	785
35	5334	98396	tgctcattagGTATCC	192	TGATTGgtaggtctgc	6010[h,i]
36	5526	104598	gctccatcagGCCCCA	188	GATCAGgtactcagag	1383
37	5714	106169	gctttctcagGATGGG	193	ACTCTGgtgggtgact	1780
38	5907	108142	tttttttttagAAGCCG	183	AGACATgtatggaatg	2686
39	6090	111011	cctcctgcagCTTCTC	182	AGGCAGgtaatgtgct	818
40	6272	112011	cttttatcagATCTTA	147	TCAGAGgtgggtggcc	383
41	6420	112541	tcctcctcagAGTCCA	197	GAAGGGgtgggtttgt	103
42	6617	112841	tctgcactagGCCCAG	231	AAACCAgtaggtgaac	1158
43	6848	114230	tcctctccagCTCCCT	139	TTGCAGgtcagtacat	1299
44	6987	115668	ccttccgcagGACAAG	144	ACACAGgtgtcttttt	4619
45	7131	120431	ttaaattcagATGATG	143	CTTGAGgtacagccat	3652
46	7274	124226	gtctgcccagGCTGCT	268	TGCCTGgtacttcgtt	97
47	7542	124591	cctctcttagGTGTGG	137	TCCATGgtcagtgcct	558
48	7679	125286	tttcttgcagTCTACT	99	ATTCAGgtgagtaatt	2686
49	7778	128071	ttaattctagGTGGGA	169	TTATAGgtgagcacat	97
50	7947	128337	acatctgtagGCTATC	126	TGAAAGgtaatattat	1808
51	8073	130271	tctgtcctagCTTTCA	109	GGTTACgtgagttatt	106
52	8182	130486	ttacaaatagGTGTGA	140	AACCAGgtatggcaga	>2015
53	8322	348	cacgaaatagGTCAGT	191	GGAAAGgtagcatcta	>800
54	8513		ttttctaaagCACTGG	106	TGTCAGgtaattcagt	82
55	8619		tttttcctagGTGGAA	92	ACAGAGgtaagtagct	>1200
56	8711		ttgtgtctagTATCAC	176	CGGAAGgtgagaacca	>1200
57	8887		gtttggttagCCTCAT	112	TCCAAGgtacggcctg	>1150
58	8999		tctgttgtagATAAAG	82	TTGCAGgtatgattat	110
59	9081		ttccttgcagTGACTG	144	ACTCAGgtacaagcca	>1100
60	9225		aatgttgcagGTGGCC	91	CAGAATgtaagggtac	291
61	9316		cttgttgtagGAACTG	178	AAAATGgtgattatac	181
62	9494		aattgagtagGTGAAA	82	ATGAAGgtgagtggct	86
63	9576		ttaaacctagGTTTGG	172	GACATGgtacgtaaac	>1000
64	9748		cttctctcagGGGAAA	145	GGGCAGgtaaggctgc	891
65	9893		tcgtaaacagGTGTAT	226	ACTTAGgtaacacaga	>1280

Table 1. (*Continued*)

Exon no.	cDNA position[a]	Exon first base[b]	Intron–exon boundary	Exon size	Exon–intron boundary	Intron size[c]
66	10119		cctcttatagGCGTGC	172	TGCCAGgtaggcttct	893
67	10291		gtcctgacagAGATGC	184	AGAGAGgtaaaagcga	578
68	10475		cttggactagATTGTT	141	AAAGAGgtgaagaggc	>1260
69	10616		tttgacttagGATGTT	192	CCACAGgtgagtctca	>1070
70	10808		tcctgaccagGTGGCA	154	TACCAGgtacaggggc	>6385
71	10962		tgtccttcagGTGCAG	108	GGTCAGgtaaggacag	1433
72	11070		cctcccgcagGCCGAG	132	CTGCTGgtaaggaagg	436
73	11202		tcattcacagGCCCTA	159	CCCTAGgtaaatgcca	85
74	11361		ctcatttcagCTGCCA	119	GCTTTGgtatggagca	904
75	11480		gtctccttagAGTTCT	126	TTTAAGgtaatgtttc	434
76	11606		gtgcctgcagGTACTG	156	GATGAGgtattgcatg	392
77	11762		ttttgtttagGTGGCT	116	GAACAGgttattatat	101
78	11878		tgtattgtagGCGACC	199	GGGAAGgtaagagctc	>12000
79	12077		cttttcttagCTGTAT	215	CAGAAGgtatgatgtg	>4000
80	12292		ttttttgcagTCCGTG	178	AAGCTGgtgaggaggc	391
81	12470		ttctctgaagGTGGAG	162	ATGAAGgtatttccca	1507
82	12632		ccccctctagATTGAT	92	TACCTGgtacgcaaga	200
83	12724		ttgtgtgcagGGGCAA	140	AGGATGgtaggtaggg	4971
84	12864		cttcattcagGTGAGG	188	GCACAGgtgagtccgg	770
85	13052		tgtgttctagGTCCCC	198	GGAAAGgtattcaagt	2606
86	13250		tgtgttttagGAGGCG	84	ATCCAGgtagcacatg	>5000
87	13334		tcctctccagGTCAAA	142	TTGTGGgtgagaactt	>200
88	13476		tcccctgcagGTGAAT	195	TCCTGGgtgagctact	>2700
89	13671		gaatgatcagGTGTGT	113	AGTGAGgtaactccct	627
90	13784		tccttaaaagGTTGAT	191	CTATAGgttggtggtc	935
91	13975		tttcttccagACTCCA	106	ACGATGgtatgccgac	290
92	14081		cctcccgcagGTGTGT	213	ATCCAGgtaggctcct	1035
93	14294		tgctcaacagGTGTTG	997	TGACATaaaagtgtag[j]	

[a] GenBank accession no. AF071172 (Ji et al. 1999).
[b] Exons 1–52, GenBank accession no. AC004583 (PAC 778A2; exon 53, GenBank accession no. AQ388928 (BAC R-142A11 end).
[c] (>) Minimum intron size based on contiguous flanking sequence.
[d] $(TA)_{22}$ begins at position 25031[b].
[e] $(CA)_{15}$ begins at position 28775[b].
[f] $(TG)_{18}$ begins at position 47153[b].
[g] $(PuT)_{66}$ begins at position 81120[b]. Pu = purine, with $(GT)_{20}$ the longest pure repeat.
[h] $(TCTG)_{5}$ begins at position 102604[b].
[i] $(TG)_{20}$ begins at position 102638[b].
[j] Polyadenylation takes place within or just 5′ of the four underlined adenine residues.

from *HERC2P2–3* have retained intron 40, with six copies of the VNTR, whereas *HERC2P1* has five VNTR copies. We noticed previously that the 3′ ends of these cDNAs do not match *HERC2* cDNA sequence (Ji et al. 1999), nor do they contain intron 52 sequence, which suggests that the 3′ ends originate from sequence homologous to a 3′-*HERC2* intron not covered by contiguous sequence (see below for origin of this sequence).

The sequence (AC002041) of a 234-kb BAC clone that maps to chromosome 16p11.2, and contains *HERC2P4*, has a contiguous 36.6-kb segment (from 50.8 kb to 87.4 kb) homologous to *HERC2*, including exons 24–42 (Fig. 1b). There are several deletions of 5′ *HERC2* that include exons 3, 5–7, and 11–23 and flanking intron sequences. The genomic sequence of *HERC2P4* also contains sequence homologous to the *HERC2* CpG island, with exon 1 and 2, as well as exons 4 and 8–10 present, which is the same pattern as the cDNA representing *HERC2P2* (Fig. 1b). This suggests that missing exons in the *HERC2P1–3* cDNAs do result from genomic deletions, as we suggested previously (Ji et al. 1999), and not from alternative splicing (Christian et al. 1999). The last 8891 bp of sequence (AC006352) of a newly identified 126-kb BAC is homologous to *HERC2* between exons 36 and 42 (Fig. 1b), in reverse orientation (an overlapping clone is needed to characterize the 5′ end of this paralog). This clone represents the putative second chromosome 16 locus (*HERC2P5*) based on the presence of identical diagnostic nucleotide sequences (Buiting et al. 1998; Ji et al. 1999). Both chromosome 16 loci have only three copies of the intron 40 VNTR. The homology of both chromosome 16 loci to *HERC2* stops in intron 42 at an identical nucleotide. An L1 element is present in both chromosome 16 loci, but not in *HERC2*, immediately after the homologous sequence. The *HERC2*-related sequences between the two chromosome 16 loci are

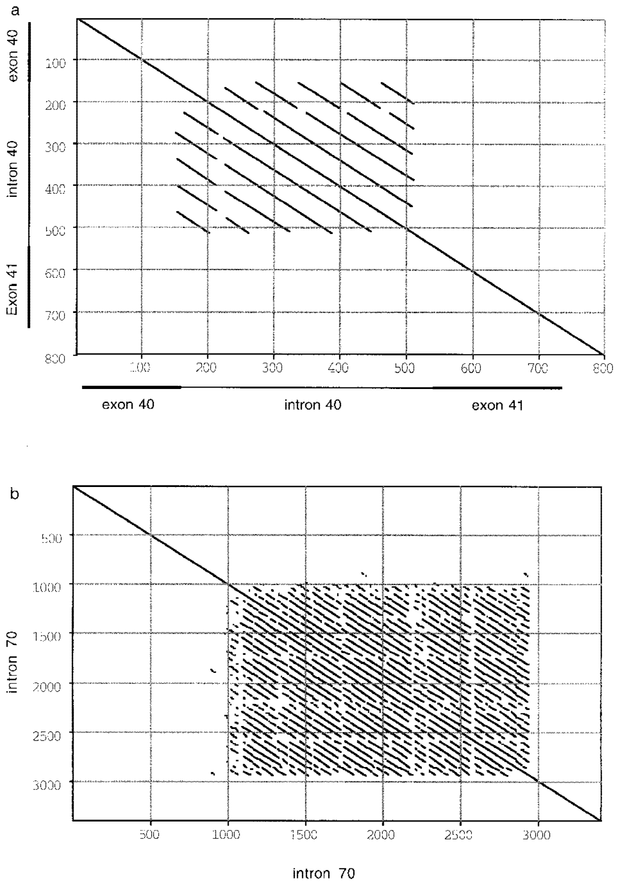

Figure 2 Analysis of putative VNTRs in *HERC2* intron 40 (*a*) and intron 70 (*b*). (*a*) Eight hundred base pairs of sequence (PAC 778A2, 112001–112800) is aligned against itself. Position 11–157 corresponds to exon 40, and 541–737 corresponds to exon 41. (*b*) The first 3400 bp of sequence from contig 27 (BAC 263O22) is aligned against itself. The parameters used for both analyses were a window of 30 nucleotides containing no less than 65% identity.

99.64% identical, which is consistent with allelism; however, the flanking 60.5 kb of sequence shared between the two chromosome 16 BAC clones have a significantly lower (98.46%) sequence identity (E.E. Eichler, pers. comm.), suggesting that the two loci are paralogous and that they diverged from an ancestral sequence near the time of divergence of chimpanzee and human (~6 mya; Goodman 1999). Therefore, either the *HERC2*-related sequence in one of the two chromosome 16 paralogous loci is of recent evolutionary origin, or gene conversion within *HERC2*-related sequence has led to homogenization of these sequences.

Two other related loci have been partially sequenced previously (*HERC2P6* and *P7*; Amos-Landgraf et al. 1999). *HERC2P6* (AF140516, AF140517) contains homologs of exons 18–20 with flanking intronic sequences, but this locus has not been further characterized. *HERC2P7* (Fig. 1b) contains homologous sequences to the *HERC2* promoter and exon 1 (AF140519), as well as intron 9 and exons 18–20 (AF140518). This locus has intron 9 joined to the 3′ half of exon 18, and the *HERC2P7* EST (AF071178) was also found to contain this fusion, with intron 18 properly spliced. Two other ESTs (AA535902, AI688214) contain this fusion. They are 98% identical to AF071178 and 99% identical to each other. This suggests that there are additional loci with such a fusion event and that the retention of intron 9 in mRNA is not an isolated event.

The sequence (AC004460) of another 114-kb genomic clone contains a duplicated segment of *HERC2* exons 63–79, excluding exon 69 (Fig. 1b). The 3′ boundary of this duplicon (denoted *HERC2P8*) may be 500 bp into intron 79, although as this is only 5 kb from the BAC end and as *HERC2* genomic sequence is not complete for this region, *HERC2P8* may contain additional 3′ sequence homologous to *HERC2*. The putative VNTR in intron 70 is present but has only 11 repeat copies. Within *HERC2P8*, 7 kb 5′ of exon 63, there is a small fragment (160 bp) homologous to *HERC2* intron 55, in the same orientation as exons 63–79, suggesting that the duplicated segment is at least 36 kb. Interestingly, we also identified homologous sequence (97%) to the 3′ end of the *HERC2P1–3* cDNAs in this clone, as two exons flank either side of the exon 63 homologous sequence but lie in the reverse orientation to *HERC2*. Each of these two sequences is flanked by consensus exon–intron boundaries, and the second of these two exons represents the last exon for the *HERC2P1–3* cDNAs, including the polyadenylation signal. These observations suggest that there has been an inversion event during the formation of the current *HERC2P1–3* duplicons, probably involving intron 52 (see above) to intron 63.

Characterization of the *Drosophila HERC2* Ortholog

Our previous studies demonstrated that the human and mouse *HERC2* cDNAs show an extraordinary 96% amino acid sequence identity (Ji et al. 1999). We extended this observation by Southern blot analysis of genomic DNA from several animal species (Fig. 3a). Under moderate hybridization conditions, *HERC2*-homologous sequences are detected in all mammals and other vertebrate species tested, as well as in the fruit fly. Nevertheless, no *HERC2* homolog is present in the sequenced genomes of *Caenorhabditis elegans* (The *C. elegans* Sequencing Consortium 1998) and *Saccharomyces cerevisiae* (Mewes et al. 1997). In contrast, database search identified a *Drosophila* EST (AA567486) highly homologous to part of the HECT domain of HERC2. Using nested primers from the 5′ end of the *Drosophila* EST and a conserved primer from the RLD3 encoded domain of human and mouse *HERC2*, we isolated additional *Drosophila HERC2* cDNA sequences

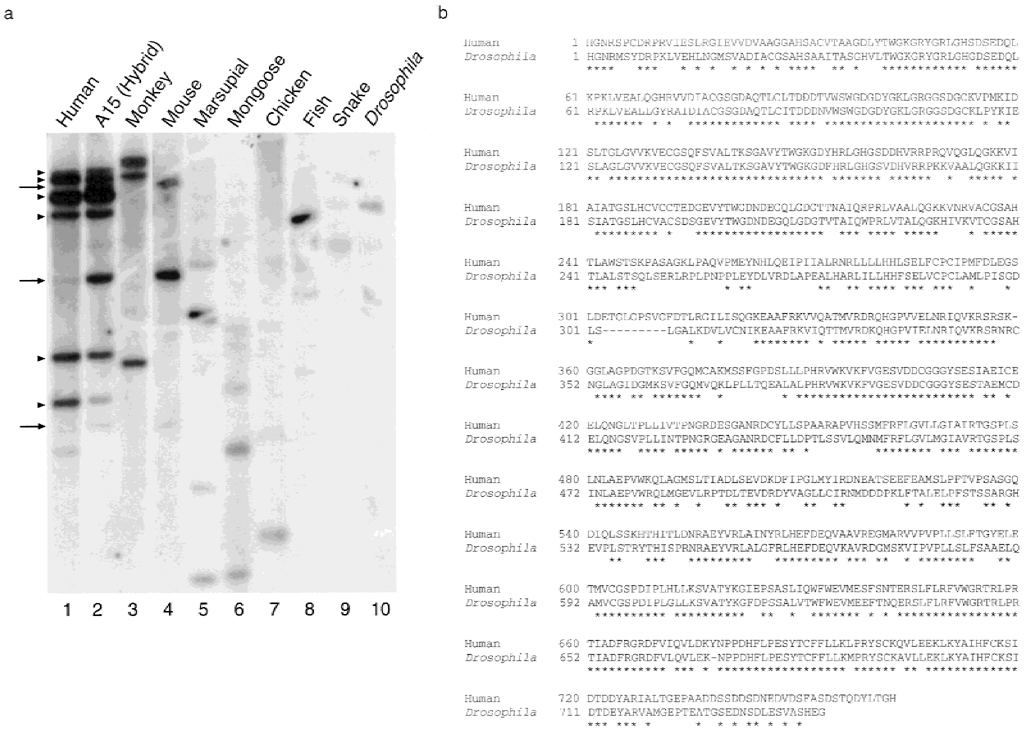

```
Human         1 HGNRSPCDRPRVIESLRGIEVVDVAAGGAHSACVTAAGDLYTWGKGRYGRLGHSDSEDQL
Drosophila    1 HGNRMSYDRPKLVEHLNGMSVADIACGSAHSAAITASGHVLTWGKGRYGRLGHGDSEDQL
                ****   ***   * * *  * * * * ****  ** *   ************ ******

Human        61 KPKLVEALQGHRVVDIACGSGDAQTLCLTDDDTVWSWGDGDYGKLGRGGSDGCKVPMKID
Drosophila   61 RPKLVEALLGYRAIDIACGSGDAQTLCITDDDNVWSWGDGDYGKLGRGGSDGCKLPYKIE
                 ******* * *  ************* **** ********************* * **

Human       121 SLTGLGVVKVECGSQFSVALTKSGAVYTWGKGDYHRLGHGSDDHVRRPRQVQGLQGKKVI
Drosophila  121 SLAGLGVVKVECGSQFSVALTKSGAVYTWGKGDFHRLGHGSVDHVRRPKKVAALQGKKII
                ** ****************************** ******* ******  *  ***** *

Human       181 AIATGSLHCVCCTEDGEVYTWGDNDEGQLGDGTTNAIQRPRLVAALQGKKVNRVACGSAH
Drosophila  181 SIATGSLHCVACSDSGEVYTWGDNDEGQLGDGTVTAIQWPRLVTALQGKHIVKVTCGSAH
                 ********* *   ******************  *** **** *****    * *****

Human       241 TLAWSTSKPASAGKLPAQVPMEYNHLQEIPIIALRNRLLLLHHLSELFCPCIPMFDLEGS
Drosophila  241 TLALSTSQLSERLRPLPNPPLEYDLVRDLAPEALHARLILLHHFSELVCPCLAMLPISGD
                *** ***            * **         **  ** **** *** ***  *    *

Human       301 LDETCLCPSVCFDTLRGILISQGKEAAFRKVVQATMVRDRQHGPVVELNRIQVKRSRSK-
Drosophila  301 LS---------LGALKDVLVCNIKEAAFRKVIQTTMVRDKQHGPVTELNRIQVKRSRNRC
                *             *   *    ******** * ***** ***** ***********

Human       360 GGLAGPDGTKSVFGQMCAKMSSFGPDSLLLPHRVWKVKFVGESVDDCGGGYSESIAEICE
Drosophila  352 NGLAGIDGMKSVFGQMVQKLPLLTQEALALPHRVWKVKFVGESVDDCGGGYSESTAEMCD
                 **** ** *******  *        * ************************* ** *

Human       420 ELQNGLTPLLIVTPNGRDESGANRDCYLLSPAARAPVHSSMFRFLGVLLGIAIRTGSPLS
Drosophila  412 ELQNGSVPLLINTPNGRGEAGANRDCFLLDPTLSSVLQMNMFRFLGVLMGIAVRTGSPLS
                *****  **** ***** * ****** ** *         ******** *** *******

Human       480 LNLAEPVWKQLAGMSLTIADLSEVDKDFIPGLMYIRDNEATSEEFEAMSLPFTVPSASGQ
Drosophila  472 INLAEPVWRQLMGEVLRPTDLTEVDRDYVAGLLCIRNMDDDPKLFTALELPFSTSSARGH
                 ******* ** *  *   ** *** *   **  **        * *  ***   ** *

Human       540 DIQLSSKHTHITLDNRAEYVRLAINYRLHEFDEQVAAVREGMARVVPVPLLSLFTGYELE
Drosophila  532 EVPLSTRYTHISPRNRAEYVRLALGFRLHEFDEQVKAVRDGMSKVIPVPLLSLFSAAELQ
                   **   ***   *********   ********* *** **  * ********   **

Human       600 TMVCGSPDIPLHLLKSVATYKGIEPSASLIQWFWEVMESFSNTERSLFLRFVWGRTRLPR
Drosophila  592 AMVCGSPDIPLGLLKSVATYKGFDPSSALVTWFWEVMEEFTNQERSLFLRFVWGRTRLPR
                 ********** **********  **  *  ******* * * *****************

Human       660 TIADFRGRDFVIQVLDKYNPPDHFLPESYTCFFLLKLPRYSCKQVLEEKLKYAIHFCKSI
Drosophila  652 TIADFRGRDFVLQVLEK-NPPDHFLPESYTCFFLLKMPRYSCKAVLLEKLKYAIHFCKSI
                *********** *** * ******************* ****** ** ************

Human       720 DTDDYARIALTGEPAADDSSDDSDNEDVDSFASDSTQDYLTGH
Drosophila  711 DTDEYARVAMGEPTEATGSEDNSDLESVASHEG
                *** *** *      *  * * ** * * *
```

Figure 3 Identification of an evolutionary highly conserved *Drosophila HERC2* gene. (*a*) Zooblot analysis of *HERC2*. A15 is a mouse–human somatic cell hybrid of which the only retained human chromosome is chromosome 15. (Monkey) African green monkey; (marsupial) *Sminthopsis macroura*. Arrows or arrowheads indicate bands in A15 that are of mouse or human origin, respectively. (Lanes *1–3*) A 3-day autoradiograph exposure; (lanes *4–10*) a 7-day exposure. (*b*) Amino acid sequence comparison of the carboxy-terminal 762 residues of human HERC2 with the partial *Drosophila* HERC2 (743 residues). Asterisks (*) indicate identical residues.

(see Methods). Combined, we have obtained 2945 bp of *Drosophila HERC2* cDNA, encoding a partial open reading frame (ORF) of 743 amino acids. The overall amino acid sequence identity between HERC2 and the carboxy-terminal *Drosophila* ORF is 70%, with long stretches of sequence identity between the two species (Fig. 3b).

A BLAST search using the partial *Drosophila* cDNA identified a working draft sequence from *Drosophila* BAC R30J04 (GenBank accession no. AC008338) as containing *HERC2*. *HERC2*-homologous sequences in the *Drosophila* BAC span the entire human gene, with only minor gaps, starting from residue 14 of HERC2 amino acid sequence. Sequence identity is highest in regions with functionally important motifs, including the three RCC1-like domains and the HECT domain (Ji et al. 1999). The ZZ-type zinc finger in human and mouse HERC2 (Ji et al. 1999) has degenerated in *Drosophila*, whereas the DOC domain (Grossberger et al. 1999) immediately following the zinc finger is conserved. Six introns have been identified in *Drosophila HERC2*, none of whose positions are conserved in the human ortholog. Nevertheless, the complete gene structure will not be known until the BAC sequence is completed. Based on several lines of evidence, *Drosophila HERC2* maps to band 19C–E of the X chromosome. This location for R30J04 was mapped by the Berkeley *Drosophila* Genome Project. Sequence identical to AC008338 is also present in BACs R41N19 (GenBank accession no. AC009217; 19A–C) and 48H01 (BAC end sequence; 19C1–C2). Furthermore, two STSs mapped to the same band as R30J04, Dm25C7 and Dm0500, are within the *Drosophila HERC2* gene. Finally, R30J04 also contains two known genes mapped previously to the 19C–D region, *pp4* (19C1–2; Helps et al. 1998) and *PBPRP-2* (19D; Pikielny et al. 1994).

DISCUSSION

Sequence analysis has revealed that the *HERC2* genomic locus, encoding a putative giant protein of 528 kD (Ji et al. 1999), comprises 93 exons. The only other characterized genes with >90 exons are the type VII collagen gene (*COL7A1*), with 118 exons (Christiano et al. 1994; Kivirikko et al. 1996), and the *perlecan* gene (*HSPG2*), with 94 exons (Cohen et al. 1993). The largest gene identified in chromosome 22 sequence has only 54 exons (Dunham et al. 1999). Therefore, with the possible exception of the 3-megadalton titin protein that is uncharacterized at the genomic level, the number of exons in *COL7A1*, *HSPG2*, and *HERC2* may represent the upper limit that a gene can have. This maximum size may result from the accuracy and time with which splicing can occur for such highly fragmented genes. Interestingly, ENU mutagenesis studies suggest that *Herc2* is the most mutable mouse locus studied so far (Walkowicz et al. 1999; E.M. Rinchik, pers. comm.). This may be due to the large number of exon–intron boundaries, because the mouse gene is likely to have the same structure, or to the large target size of the 15.3-kb *Herc2* exons and encoded ORF. We have identified three splice site mutations in ENU-generated *jdf2* animals (Ji et al. 1999). Alternatively, the exceptionally high mouse–human identity suggests that even minor changes of HERC2 amino acid sequence could lead to dysfunction of the protein, consistent with the high rate of ENU mutation.

Recently, Shiraishi et al. (1999) isolated DNA fragments representing methylated CpG islands in human adenocarcinomas of the lung, one (AB077148) that is 99% identical to the *HERC2* CpG island promoter. A PCR-based investigation of methylation status of AB077148 in genomic DNA showed differential methylation in both cancerous and noncancerous lung tissue of the same patients, suggesting it may be imprinted (Shiraishi et al. 1999). However, *HERC2* is expressed from both maternal and paternal alleles and hence is not imprinted in either human or mouse (Gabriel et al. 1998, 1999; Ji et al. 1999). Consistent with this, *Herc2* mutations in the *jdf2* syndrome are recessive (Lehman et al. 1998; Ji et al. 1999). The differential methylation observed by Shiraishi et al. (1999) could result from an inability of the PCR-based assay to distinguish the *HERC2* promoter and the estimated nine additional duplicated copies (Amos-Landgraf et al. 1999; this paper). Because at least four copies of *HERC2*-related CpG islands are pericentromeric in 15q11.1 and 16p11, these may be methylated. Alternatively, it is possible that the “noncancerous tissue” (Shiraishi et al. 1999) is actually precancerous and that *HERC2* and/or related sequences may be targets of silencing by methylation during tumorigenesis.

The *HERC2* gene is evolutionary highly conserved, with human and *Drosophila* HERC2 showing 70% identity over the carboxy-terminal 743 amino acids. Further analysis of *Drosophila HERC2* genomic sequence suggests that much of the protein is functionally important, particularly the three RCC1-like domains and the HECT domain. In contrast, the ZZ zinc finger (Ji et al. 1999) is not present in the fly HERC2, suggesting some differences in protein–protein interactions compared with human HERC2. The high degree of homology across mammalian and invertebrate species indicates that HERC2 plays a conserved role in the cell. Identification of mutations in *Drosophila HERC2*, based on chromosomal location, may allow comparison to the *jdf2* mice to better understand the developmental function of HERC2, which may help predict more accurately the potential human phenotype expected for *HERC2* mutations.

In the finished genomic sequence, the only gene identified other than *HERC2* was a processed pseudogene (*RPL41P2*), inserted into an *Alu* element in *HERC2* intron 2. Although it is unknown whether the two putative VNTRs identified within *HERC2* are polymorphic in human populations, this appears likely as there is variation between the copy number of both VNTRs in *HERC2* and that for *HERC2*-containing duplicons. Most copies of the intron 40 VNTR contain exon 40 coding sequence and the exon–intron boundary, although the effect on intron 40 splicing is unknown. Interestingly, this intron is not spliced in most transcripts from *HERC2P1–3*, despite retention of five to six VNTR copies. The large VNTR in intron 70 is preceded by a CpG-rich region. The same genomic region in mouse has been suggested to contain a regulatory element for *p* gene expression (Walkowicz et al. 1999). It is possible that this VNTR, together with the CpG island, has this function in mouse and human. However, further studies in the mouse and analysis of whether transcripts are produced from the intronic CpG island will be necessary to determine its function.

Previous evidence suggests that there are seven *HERC2*-containing duplicons in 15q11, including five with a copy of the *HERC2* 5′ CpG island and two copies that do not have the CpG island but contain other 5′ sequences (Amos-Landgraf et al. 1999). Similarly, three duplicons in 15q13 each carry the 5′ CpG island (Amos-Landgraf et al. 1999), the most proximal of which is the ancestral *HERC2* gene (Ji et al. 1999). Our previous (Buiting et al. 1998; Amos-Landgraf et al. 1999) and current studies also define two *HERC2*-containing duplicons in chromosome 16p11.2, for a total of 12 loci containing sequence from the 5′ half of *HERC2*. Although exon 93 of *HERC2* is unique in the human genome (Ji et al. 1999), we demonstrated here that *HERC2P8* contains sequences paralogous to intron 55 to exon 79, in the absence of further 5′ sequences, suggesting that there are even more than 12 *HERC2* duplicons in the genome. However, many of these duplicons may be highly fragmented and represent distinct subfamilies. Christian et al. (1999) independently identified duplicons at or near the proximal and distal PWS/AS breakpoints, by STS content mapping in YACs and by interphase FISH. Proximal breakpoint 2 (15q11) was suggested to be a single duplicon of ~400 kb in size, in inverted orientation to two duplicon copies in 15q13 (Christian et al. 1999). However, these studies cannot discriminate between closely related and closely spaced repeats, nor divergent copies; hence, we suggest that these studies have underestimated the number of duplicons in the breakpoint regions. Our results indicate that one end of the *END* repeat duplicons is within 3′ HERC2 (between exons 79 and 93).

The *HERC2*-related content is 36.6 kb in the most rearranged/deleted duplicon in 16p11.2, but *HERC2* sequences from exon 1 to at least exon 79 (spanning 150–200 kb) are included in some chromosome 15 duplicons. However, the endpoint of the duplicon 5′ of *HERC2* is unknown at this time. Christian et al. (1999) identified five ESTs and two PAC ends homologous to genes within the duplicated regions, which suggests that additional genes or pseudogenes may be present in the duplicons or that several classes of unrelated duplicons may be interspersed in these regions. However, not all these ESTs represent new genes. One EST (A006B10) is from a duplicated *HERC2* locus, and a second (A008B26) is homologous to *HERC2* intron 4 (and corresponds to an L1 element). According to their putative map positions (Christian et al. 1999), the two PAC-end gene sequences should be within the 3′ end of the *HERC2* locus and may lie in unfinished intronic regions, perhaps adjacent to the CpG island in intron 70. This leaves three potential genes within the *END* repeats outside and telomeric of *HERC2*. One is *MYLE*, a 1-kb transcript encoding a putative 68-amino-acid protein, whereas the other two ESTs (SHGC17218 and SGC32610) have not been characterized. Taken together, duplicons in the PWS/AS deletion breakpoint regions are clearly complex in structure and arrangement, with *HERC2* a major component. It will, however, be necessary to build and sequence complete clone contigs of these duplicons to gain a full understanding of the complexity of these sequences.

We have shown previously that a stable putative fusion *HERC2* to *HERC2*-related transcript could be detected by Northern analysis in one of five PWS/AS deletion patients (Amos-Landgraf et al. 1999). Given that distal breakpoints could also occur in *HERC2*-related sequences telomeric of *HERC2* and that some fusion genes may not produce stable transcripts, many PWS/AS deletion breakpoints may occur within the *HERC2*-related portions of the *END* repeats. The newly identified microsatellite and VNTR sequences within *HERC2* should help identify the positions of PWS/AS breakpoints within or distal to *HERC2*. Similar studies will also determine the potential role of *HERC2*-containing duplicons in other chromosome 15q11–q13 rearrangements, including duplications (Clayton-Smith et al. 1993a; Browne et al. 1997; Repetto et al. 1998), triplications (Schinzel et al. 1994; Cassidy et al. 1996), inversions (Clayton-Smith et al. 1993b), and inverted duplications [inv dup(15)] (Robinson et al. 1993; Huang et al. 1997; Wandstrat et al. 1998). Other chromosome-specific duplicons are implicated in many additional chromosomal rearrangements (Lupski 1998; Y. Ji, E. Eichler, S. Schwartz, and R.D. Nicholls, in prep). Although some involve a simple, low-copy repeat, others show a complexity comparable to the duplicons we have described in 15q11, 15q13, and 16p11 (Y. Ji, E. Eichler, S. Schwartz, and R.D. Nicholls, in prep). For example, four genes occur in the large (>200-kb) duplicons mediating the deletion in Smith–Magenis syndrome (Chen et al. 1997). Duplicons in chromosome 22q11 (LCR22s) are also very complex, with eight copies of the LCR22s ranging from ~20 kb to >200 kb (Dunham et al. 1999; Edelmann et al. 1999a,b). Multiple genes/pseudogenes map within each of the LCR22 duplicons (Collins et al. 1997; Dunham et al. 1999; Edelmann et al. 1999a,b), with duplications, deletions, and inverted duplications predominantly mediated by three of these duplicons (Edelmann et al. 1999b). The mechanism in homologous chromosome rearrangements involving simple duplicons (Y. Ji, E. Eichler, S. Schwartz, and R.D. Nicholls, in prep.) is now thought to involve double-strand break repair (Lupski 1998; Lopes et al. 1999), but the mechanisms in cases involving complex duplicons are not known as breakpoints have not been characterized. Further studies of complex duplicons will determine how and why these sequences are genetically unstable in both evolutionary terms of expansion and dispersal, and their role in mediating chromosome rearrangements in genetic diseases.

METHODS

Isolation of PAC and BAC Clones

We screened a human genomic PAC library (RPCI-4) with a 1.1-kb *HERC2* cDNA probe (probe C, cDNA coordinates 2612–3714; Ji et al. 1999) using standard hybridization and washing conditions (Church and Gilbert 1984) and isolated a total of 30 positive clones. These may represent six or more different loci because the library has a fivefold coverage of the human genome and probe C contains a 5′ region of *HERC2* that is duplicated. PCR primers RN304 (Ji et al. 1999) and RN305 (5′-ACCAGCCACTCTGCAGCACG-3′) were used to amplify a 107-bp STS (which corresponds to part of exon 18 of *HERC2*) from seven of the PAC clones, and the products were cloned into the pCR2.1 vector (Invitrogen, Carlsbad, CA) and sequenced. Five contained sequence identical to *HERC2P6* (λ6A1; Ji et al. 1999), one identical to *HERC2P7* (λ11A1; Ji et al. 1999), and PAC 778A2 has the same sequence as *HERC2* cDNA. An *Eag*I sequence variant present in *HERC2* but not *HERC2P6* nor *HERC2P7* was identified in this STS. Based on STS PCR and *Eag*I digestion, none of the remaining 23 PACs contain sequence identical to *HERC2*.

Two STSs were used to screen by PCR the RPCI-11 human BAC library (Research Genetics, Huntsville, AL). A single positive clone (263O22) was isolated using a 171-bp STS [primers RN638 (5′-TCGTGAGTCGTCTTGATTGTAT-3′, starts from nucleotide 14940 of *HERC2* cDNA) and RN637 (5′-CTTCTGGTTTTTCATTTTGGTT-3′, ends in nucleotide 15110)] from the unique 3′ UTR of *HERC2* (Ji et al. 1999). Multiple positive genomic clones were isolated using primers RN911 (5′-GTTTGGTATTTTCCTGGGGTGATG-3′) and RN912 (5′-ACCCCCTGTCCATTTAGTCTCTCA-3′), which corresponds to a duplicated portion of *HERC2* cDNA sequence (9576–9681) (see Results). Only one (361F20) was also positive for the *HERC2* 3′ UTR and hence is derived from the

HERC2 locus. By screening the TIGR BAC-end database (http://www.TIGR.ORG) with *HERC2* cDNA sequence, we identified R-142A11 as positive for *HERC2* exon 53 (see Results), and further characterization of this BAC showed that it is also positive for the *HERC2* 3′ UTR.

Other STS primers used for typing PACs and BACs in this study include RN599 (5′-ACTGGACTGGGTTGCTATCAGAAAT-3′) and RN600 (5′-CACAAAAATCAAAGTCATCACAGTTT C-3′) for *HERC2* exons 51–52 and RN687 (5′-AGTGATGGGTCTGTGAATGG-3′) and RN690 (5′-TTCCCCATCATTTTCTCCCAGCAG-3′) for *HERC2* exons 72–74, as well as primers for exons of the *P* gene (Lee et al. 1995).

Sequence Analysis of *HERC2* Genomic Clones and Related Sequences

PAC 778A2 and BAC 263O22 were shotgun subcloned into an M13 phage vector and sequenced. PAC 778A2 sequence was finished, whereas BAC 263O22 was only partially sequenced and assembled into 22 contigs of at least two overlapping sequence reads. From the latter sequence, 22 exons were identified, including *HERC2* exons 70–93 with the exception of exons 80 and 88. *P* exon 3 is present in one 263O22 sequence contig. Both ends of BAC R-142A11 were sequenced (Cleveland Genomics, Cleveland, OH). To identify exon–intron boundaries for exons 54–69, as well as exons 80 and 88, primers were designed from *HERC2* cDNA sequence (primer sequences available from the corresponding author) and used to directly sequence from BAC clones R-142A11 and 263O22 (Cleveland Genomics).

HERC2 exons and polymorphisms were identified by pairwise sequence alignment (http://dot.imgen.bcm.tmc.edu:9331) of genomic sequence with *HERC2* cDNA sequence (GenBank accession no. AF071172; Ji et al. 1999). RepeatMasker (http://ftp.genome.washington. edu/cgi-bin/RepeatMasker) was used to analyze genome-wide repetitive elements and simple repeats and to calculate repeat and GC contents. The MacVector software package was used to characterize the VNTR sequences. EST and gene homologs were identified using BLAST (http://www.ncbi.nlm.nih.gov/cgi-bin/BLAST/nph-newblast). BLAST and pairwise sequence alignments were used to analyze the duplicated *HERC2* loci.

Analysis of *Drosophila HERC2*

Southern hybridization of zooblots was performed by standard methods (Sambrook et al. 1989), with probe C (Ji et al. 1999), using 30% formamide prehybridization and hybridization solutions, and a final wash at 45°C with 2× SSC and 0.1% SDS. A *Drosophila* EST (GenBank accession no. AA567486) homologous to 3′ *HERC2* was identified in the dbEST database by BLAST. Sequence analysis revealed a 1372-bp cDNA fragment, with a 661-bp ORF and a 3′ UTR of 711 bp. Two nested primers were designed from the 5′ end of this clone and used, together with a human *HERC2* primer (RN667; Ji et al. 1999), to PCR amplify an additional 5′ cDNA from an oocyte SMART cDNA library (Clontech, Palo Alto, CA). Primers RN808 (5′-GAGAGCAAAGGCACTGGAATCACC-3′) and RN667 were used for first-round PCR (annealing at 55°C for 30 sec and extension at 68°C for 2 min), then RN807 (5′-TTCCTGGGCGAGATGTGCGTGTAG-3′) and RN667 were used for nested PCR (annealing at 60°C for 30 sec, and extension at 72°C for 2 min). PCR was performed with the Advantage cDNA PCR Kit (Clontech); the 1.6-kb nested PCR product was cloned into the pCR2.1 vector (Invitrogen) and sequenced. A BLAST search of the High Throughput Genomic Sequences database, using compiled *Drosophila HERC2* cDNA sequence, identified BAC R30J04 (GenBank accession no. AC008338) as containing *Drosophila HERC2*. BLAST searches and pairwise sequence alignments, using the human HERC2 protein sequence and AC008338 translated in all six frames, identified additional amino-terminal *Drosophila* HERC2 sequences in this BAC.

ACKNOWLEDGMENTS

We thank Drs. Todd A. Gray and Evan E. Eichler for helpful discussions, James M. Amos-Landgraf and Tao Pan for technical contributions, and Drs. Evan E. Eichler and Peter J. Harte for critical reading of the manuscript. This work was funded by a Neuromuscular Disease Research Program Grant from the Muscular Dystrophy Association (R.D.N.) and the National Institutes of Health (R.A.S.).

The publication costs of this article were defrayed in part by payment of page charges. This article must therefore be hereby marked "advertisement" in accordance with 18 USC section 1734 solely to indicate this fact.

REFERENCES

Amos-Landgraf, J.M., Y. Ji, W. Gottlieb, T. Depinet, A. Wandstradt, S.B. Cassidy, D.J. Driscoll, P.K. Rogan, S. Schwartz, and R.D. Nicholls. 1999. Chromosome breakage in the Prader-Willi and Angelman syndromes involves recombination between large, transcribed repeats at proximal and distal breakpoints. *Am. J. Hum. Genet.* **65:** 370–386.

Bird, A.P. 1986. CpG-rich islands and the function of DNA methylation. *Nature* **321:** 209–213.

Browne, C.E., N.R. Dennis, E. Maher, F.L. Long, J.C. Nicholson, J. Sillibourne, and J.C.K. Barber. 1997. Inherited interstitial duplications of proximal 15q: Genotype-phenotype correlations. *Am. J. Hum. Genet.* **61:** 1342–1352.

Buiting, K., S. Gross, Y. Ji, G. Senger, R.D. Nicholls, and B. Horsthemke. 1998. Expressed copies of the MN7 (*D15F37*) gene family map close to the common deletion breakpoints in the Prader-Willi/Angelman syndromes. *Cytogenet. Cell Genet.* **81:** 247–253.

Cassidy, S.B., J. Conroy, L. Becker, and S. Schwartz. 1996. Paternal triplication of 15q11-q13 in a hypotonic, developmentally delayed child without Prader-Willi or Angelman syndrome. *Am. J. Med. Genet.* **62:** 206–207.

The *C. elegans* Sequencing Consortium. 1998. Genome sequence of the nematode *C. elegans*: A platform for investigating biology [published erratum appears in *Science* 1998 **283** 35]. *Science* **282:** 2012–2018.

Chen, K.S., P. Manian, T. Koeuth, L. Potocki, Q. Zhao, A.C. Chinault, C.C. Lee, and J.R. Lupski. 1997. Homologous recombination of a flanking repeat gene cluster is a mechanism for a common contiguous gene deletion syndrome. *Nat. Genet.* **17:** 154–163.

Christian, S.L., J.A. Fantes, S.K. Mewborn, B. Huang, and D.H. Ledbetter. 1999. Large genomic duplicons map to sites of instability in the Prader-Willi/Angelman syndrome chromosome region (15q11-q13). *Hum. Mol. Genet.* **8:** 1025–1037.

Christiano, A.M., G.G. Hoffman, L.C. Chung-Honet, S. Lee, W. Cheng, J. Uitto, and D.S. Greenspan. 1994. Structural organization of the human type VII collagen gene (*COL7A1*), composed of more exons than any previously characterized gene. *Genomics* **21:** 69–79.

Church, G.M. and W. Gilbert. 1984. Genomic sequencing. *Proc. Natl. Acad. Sci.* **81:** 1991–1995.

Clayton-Smith, J., T. Webb, X.J. Cheng, M.E. Pembrey, and S. Malcolm. 1993a. Duplication of chromosome 15 in the region

15q11-13 in a patient with developmental delay and ataxia with similarities to Angelman syndrome. *J. Med. Genet.* **30:** 529–531.

Clayton-Smith, J., D.J. Driscoll, M.F. Waters, T. Webb, T. Andrews, S. Malcolm, M.E. Pembrey, and R.D. Nicholls. 1993b. Difference in methylation patterns within the *D15S9* region of chromosome 15q11-q13 in first cousins with Angelman syndrome and Prader-Willi syndrome. *Am. J. Med. Genet.* **47:** 683–686.

Cohen, I.R., S. Grassel, A.D. Murdoch, and R.Y. Iozzo. 1993. Structural characterization of the complete human perlecan gene and its promoter. *Proc. Natl. Acad. Sci.* **90:** 10404–10408.

Collins, J.E., A.J. Mungall, K.L. Badcock, J.M. Fay, and I. Dunham. 1997. The organization of the γ-glutamyl transferase genes and other low copy repeats in human chromosome 22q11. *Genome Res.* **7:** 522–531.

Dunham, I., N. Shimizu, B.A. Roe, S. Chissoe, A.R. Hunt, J.E. Collins, R. Bruskiewich, D.M. Beare, M. Clamp, L.J. Smink et al. 1999. The DNA sequence of human chromosome 22. *Nature* **402:** 489–495.

Edelmann, L., R.K. Pandita, and B.E. Morrow. 1999a. Low-copy repeats mediate the common 3-Mb deletion in patients with velo-cardio-facial syndrome. *Am. J. Hum. Genet.* **64:** 1076–1086.

Edelmann, L., R.K. Pandita, E. Spiteri, B. Funke, R. Goldberg, N. Palanisamy, R.S. Chaganti, E. Magenis, R.J. Shprintzen, and B.E. Morrow. 1999b. A common molecular basis for rearrangement disorders on chromosome 22q11. *Hum. Mol. Genet.* **8:** 1157–1167.

Gabriel, J.M., M.J. Higgins, T.C. Gebuhr, T. Shows, S. Saitoh, and R.D. Nicholls. 1998. A model system to study genomic imprinting of human genes. *Proc. Natl. Acad. Sci.* **95:** 14857–14862.

Gabriel, J.M., M. Merchant, T. Ohta, Y. Ji, R.G. Caldwell, M.J. Ramsey, J.D. Tucker, R. Longnecker, and R.D. Nicholls. 1999. A transgene insertion creating a heritable chromosome deletion mouse model of Prader-Willi and Angelman syndrome. *Proc. Natl. Acad. Sci.* **96:** 9258–9263.

Goodman, M. 1999. The genomic record of Humankind's evolutionary roots. *Am. J. Hum. Genet.* **64:** 31–39.

Grossberger, R., C. Gieffers, W. Zachariae, A.V. Podtelejnikov, A. Schleiffer, K. Nasmyth, M. Mann, and J.M. Peters. 1999. Characterization of the DOC1/APC10 subunit of the yeast and the human anaphase-promoting complex. *J. Biol. Chem.* **274:** 14500–14507.

Helps, N.R., N.D. Brewis, K. Lineruth, T. Davis, K. Kaiser, and P.T. Cohen. 1998. Protein phosphatase 4 is an essential enzyme required for organisation of microtubules at centrosomes in *Drosophila* embryos. *J. Cell Sci.* **111:** 1331–1340.

Huang, B., J.A. Crolla, S.L. Christian, M.E. Wolf-Ledbetter, M.E. Macha, P.N. Papenhausen, and D.H. Ledbetter. 1997. Refined molecular characterization of the breakpoints in small inv dup(15) chromosomes. *Hum. Genet.* **99:** 11–17.

Ji, Y., M.J. Walkowicz, K. Buiting, D.K. Johnson, R.E. Tarvin, E.M. Rinchik, B. Horsthemke, L. Stubbs, and R.D. Nicholls. 1999. The ancestral gene for transcribed, low-copy repeats in the Prader-Willi/Angelman region encodes a large protein implicated in protein trafficking, which is deficient in mice with neuromuscular and spermiogenic abnormalities. *Hum. Mol. Genet.* **8:** 533–542.

Kenmochi, N., T. Kawaguchi, S. Rozen, E. Davis, N. Goodman, T.J. Hudson, T. Tanaka, and D.C. Page. 1998. A map of 75 human ribosomal protein genes. *Genome Res.* **8:** 509–523.

Kivirikko, S., K. Li, A.M. Christiano, and J. Uitto. 1996. Structure of mouse type VII collagen reveals evolutionary conservation of functional protein domains and genomic organization. *J. Invest. Dermatol.* **106:** 1300–1306

Lee, S.T., R.D. Nicholls, M.T. Jong, K. Fukai, and R.A. Spritz. 1995. Organization and sequence of the human *P* gene and identification of a new family of transport proteins. *Genomics* **26:** 354–363.

Lehman, A.L., Y. Nakatsu, A. Ching, R.T. Bronson, R.J. Oakey, N. Keipo-Hrynko, J.N. Finger, D. Durham-Pierre, D.B. Horton, J.M. Newton et al. 1998. A very large protein with diverse functional motifs is deficient in rjs (runty, jerky, sterile) mice. *Proc. Natl. Acad. Sci.* **95:** 9436–9441.

Lopes, J., S. Tardieu, K. Silander, I. Blair, A. Vandenberghe, F. Palau, M. Ruberg, A. Brice, and E. LeGuern. 1999. Homologous DNA exchanges in humans can be explained by the yeast double-strand break repair model: A study of 17p11.2 rearrangements associated with CMT1A and HNPP. *Hum. Mol. Genet.* **8:** 2285–2292.

Lupski, J.R. 1998. Genomic disorders: Structural features of the genome can lead to DNA rearrangements and human disease traits. *Trends Genet.* **14:** 417–422.

Maquat, L.E. 1996. Defects in RNA splicing and the consequence of shortened translational reading frames. *Am. J. Hum. Genet.* **59:** 279–286.

Mewes, H.W., K. Albermann, M. Bahr, D. Frishman, A. Gleissner, J. Hani, K. Heumann, K. Kleine, A. Maierl, S.G. Oliver et al. 1997. Overview of the yeast genome [published erratum appears in *Nature* 1997, **387:** 737]. *Nature* (Suppl.) **387:** 7–65.

Nicholls, R.D., S. Saitoh, and B. Horsthemke. 1998. Imprinting in Prader-Willi and Angelman syndromes. *Trends Genet.* **14:** 194–200.

Nomura, N., N. Miyajima, T. Sazuka, A. Tanaka, Y. Kawarabayasi, S. Sato, T. Nagase, N. Seki, K. Ishikawa, and S. Tabata. 1994. Prediction of the coding sequences of unidentified human genes. I. The coding sequences of 40 new genes (KIAA0001-KIAA0040) deduced by analysis of randomly sampled cDNA clones from human immature myeloid cell line KG-1. *DNA Res.* **1:** 27–35.

Pikielny, C.W., G. Hasan, F. Rouyer, and M. Rosbash. 1994. Members of a family of *Drosophila* putative odorant-binding proteins are expressed in different subsets of olfactory hairs. *Neuron* **12:** 35–49.

Repetto, G.M., L.M. White, P.J. Bader, D. Johnson, and J.H.M. Knoll. 1998. Interstitial duplications of chromosome region 15q11q13: Clinical and molecular characterization. *Am. J. Med. Genet.* **9:** 82–89.

Robinson, W.P., F. Binkert, R. Gine, C. Vazques, W. Miller, W. Rosenkranz, and A. Schinzel. 1993. Clinical and molecular analysis of five inv dup(15) patients. *Eur. J. Hum. Genet.* **1:** 37–50.

Rosa, J.L. and M. Barbacid. 1997. A giant protein that stimulates guanine nucleotide exchange on ARF1 and Rab proteins forms a cytosolic ternary complex with clathrin and Hsp70. *Oncogene* **15:** 1–6.

Rosa, J.L., R.P. Casaroli-Marano, A.J. Buckler, S. Vilaro, and M. Barbacid. 1996. p619, a giant protein related to the chromosome condensation regulator RCC1, stimulates guanine nucleotide exchange on ARF1 and Rab proteins [published erratum appears in *EMBO J.* 1996, **15:** 5738]. *EMBO J.* **15:** 4262–4273.

Sambrook, J., E.F. Fritsch, and T. Maniatis. 1989. *Molecular cloning: A laboratory manual*, 2nd ed. Cold Spring Harbor Laboratory Press, Cold Spring Harbor, NY.

Schinzel, A.A., L. Brecevic, F. Bernasconi, F. Binkert, F. Berthet, A. Wuilloud, and W.P. Robinson. 1994. Intrachromosomal triplication of 15q11-q13. *J. Med. Genet.* **31:** 798–803.

Shiraishi, M., Y.H. Chuu, and T. Sekiya. 1999. Isolation of DNA fragments associated with methylated CpG islands in human adenocarcinomas of the lung using a methylated DNA binding column and denaturing gradient gel electrophoresis. *Proc. Natl. Acad. Sci.* **96:** 2913–2918.

Walkowicz, M., Y. Ji, X. Ren, B. Horsthemke, L.B. Russell, D.K. Johnson, E.M. Rinchik, R.D. Nicholls, and L. Stubbs. 1999. Molecular characterization of radiation- and chemically-induced mutations associated with neuromuscular tremors, runting, juvenile lethality, and sperm defects in *jdf2* mice. *Mamm. Genome* **10:** 870–878.

Wandstrat, A.E., J. Leana-Cox, L. Jenkins, and S. Schwartz. 1998. Molecular cytogenetic evidence for a common breakpoint in the largest inverted duplications of chromosome 15. *Am. J. Hum. Genet.* **62:** 925–936.

Received September 28, 1999; accepted in revised form January 5, 2000.